

Cite this: *RSC Adv.*, 2018, **8**, 41270

Preparation of pH-responsive asymmetric polysulfone ultrafiltration membranes with enhanced anti-fouling properties and performance by incorporating poly(2-ethyl-2-oxazoline) additive

Ruizhang Xu, ^a Jiantao Wang, ^a DanDan Chen, ^a Feng Yang, ^a Jian Kang, ^{*a} Ming Xiang, ^a Lu Li^b and Xingyue Sheng^b

Inspired by the special pH value-responsive and strong hydrophilic ability of poly(2-ethyl-2-oxazoline) (PEOX), in this study, asymmetric polysulfone (PSf) and PSf/PEOX ultrafiltration membranes were prepared by a phase separation method, wherein different dosages of PEOX (0–3 wt%) were incorporated into the PSf casting solution as polymeric additives. The effects of PEOX dosages on the phase separation kinetics, chemical properties, morphology, hydrophilicity, porosity and performances such as pure water flux (PWF), Bull Serum Albumin (BSA) rejection, pH value responsiveness and anti-fouling property were investigated in detail. The hydrophilicity, pure water flux, BSA rejection and anti-fouling property were improved significantly after the incorporation of PEOX. The PWF increased from $213.5 \text{ L m}^{-2} \text{ h}^{-1}$ to $419.8 \text{ L m}^{-2} \text{ h}^{-1}$ as the PEOX dosage increased from 0 to 1 wt%, meanwhile, the BSA rejection increased to more than 98.4%. Viscosity and effective diffusion coefficient of PSf/PEOX solution were studied to elucidate the role of PEOX in phase separation and morphology of the membrane. Results showed that the incorporation of PEOX leads to the phase separation of casting solution by making it more prone to instantaneous demixing, further determining the morphology and performances of the membrane. Interestingly, the resulting membranes showed pH value-responsive properties, whereby the water flux increased along with an increase in the pH value. This interesting feature of the membranes broadens their application potential in many specific cases. The related filtration mechanism has also been proposed.

Received 10th September 2018
Accepted 28th November 2018

DOI: 10.1039/c8ra07529h

rsc.li/rsc-advances

1. Introduction

The phase separation process is a broadly utilized strategy for the preparation of asymmetric ultrafiltration membranes.¹ Over the past few decades, such ultrafiltration membranes are widely used in many fields for the removal of impurities, toxic and harmful substances from water, and the manufacturing of industrial and medical instruments (*e.g.* fruit juice concentrator, and hemodialysis machine).² Many scientists have carried out extensive research in this field.^{3,4}

The asymmetric ultrafiltration membrane formation method and mechanism have been widely reported.^{5–9} In lab-scale, a casting solution comprising of a polymer and a solvent (for instance, a solution of PSf in DMF) is cast uniformly onto a polyester film or a glass plate substrate using a hand-casting knife with a constant gap. After the casting solution is spread

uniformly onto the substrate, the substrate is subsequently immersed into a non-solvent coagulation bath (generally, distilled water). Then, because of the low miscibility between the polymer phase and the non-solvent phase with the concurrent high miscibility between the solvent and the non-solvent, the thermodynamic instability leads to the occurrence of liquid–liquid phase separation. In this process, the solvent in the casting solution exchanges with the non-solvent across the interface between them; precipitation of polymer phase starts simultaneously. In detail, the high miscibility between the solvent and non-solvent causes a diffusional stream of the two liquids at some locations on the top surface and the sublayer of the polymer phase, and the invasion of the non-solvent into the polymer phase leads to the formation of nuclei of a polymer-poor phase (low miscibility results in the repulsion of polymer chains and water molecules). Upon continued diffusion, the nuclei grow until the polymer concentration in the non-solvent is too high and precipitation occurs, voids are formed and fixed in the process,^{10,11} and a porous asymmetric membrane with a dense top surface and a porous sublayer is obtained in this process.

^aState Key Laboratory of Polymer Materials Engineering, Polymer Research Institute of Sichuan University, Chengdu 610065, People's Republic of China. E-mail: jiankang@sru.edu.cn; Fax: +86-028-85406578; Tel: +86-028-85405347

^bChongqing Zhixiang Paving Technology Engineering Co., Ltd., Chongqing, 401336, China



The formation, the microstructure and the performance of the final ultrafiltration membrane are determined by the exchange rate between the solvent and the non-solvent, which can be controlled by changing many variables, such as the composition of polymer solution, coagulant temperature and additives.^{2,12,13} So, a membrane with satisfactory properties can be obtained by carefully controlling the phase separation conditions.^{14–16}

Adding additives is a major method to modify the properties of membranes in phase separation process. Additives affect the structures and properties of membranes by enlarging or preventing the formation of macrovoids, adjusting the pore interconnectivity, and/or changing the hydrophilicity of membranes.^{6,17–21} In the early 1960s, research on additives was mainly concerned with small molecular additives, such as an organic salt.²² On one hand, the interaction forces between the poly-molecular chains are changed by the organic salt. On the other hand, during the phase separation process, organic salt can dissociate from the polymer phase and facilitate the formation of voids.¹³

Later on, it was found that the void structure of an ultrafiltration membrane could be altered to a large extent by changing the molecular weight and the dosage of additives. Thus, polymers were considered as the new kind of additives. Hydrophilic additives such as poly(ethylene glycol) (PEG) or poly(vinyl pyrrolidone) (PVP) are the two most commonly used polymer additives, which could play an important role in the process of phase separation.^{2,23–26} However, the influences of polymer additives on the morphologies and structures of the resulting membranes are different. The polymer additives can not only induce the formation of macrovoids,^{2,25} but can also act as macrovoid suppressors.^{6,20,21,24,26–28}

Poly(2-ethyl-2-oxazoline) (PEOX) is a biodegradable (acceptable degradation rate in use²⁹) and water-soluble polymer with pH- and temperature-responsive properties.^{30,31} In an aqueous solution, PEOX has a LCST (lower critical solution temperature). When the temperature is below its LCST, PEOX would hydrate with water through hydrogen bonding, which could result in the swelling of PEOX. So, when the temperature is low, PEOX has a relatively large swelling ratio. Besides, in an aqueous solution, when the pH value is low, the amide groups in PEOX are ionized, leading to the possible aggregation of the PEOX molecular chains *via* intermolecular hydrogen bonds. While the pH value increases, the hydrogen ions dissociate from the amide groups in PEOX, which can result in the breaking of hydrogen bonds. Shrunken PEOX molecular chains will start to expand and cause it to swell. That is to say, while the pH value is high, PEOX has a relatively large swelling ratio.³¹

PEOX shows high hydrophilicity because it can combine with water *via* plenty of hydrogen bonding, thus, water is the θ solvent for PEOX.³² The hydrophilic PEOX is thought to be much better than PEG or PVP because of its high hygroscopicity. Its *N,N*-dimethylacetamide (DMAc) group is considered as a broadly compatible polymeric solvent or a compatibility agent for many polymers.³³ At the same time, PEOX is easy to dissolve in DMF.

Inspired by the interesting features of PEOX mentioned above, the addition of PEOX as an additive into the PSf solution might impart pH sensitive property to the permeation performance of the resulting PSf membranes, which has never been reported before and is of great importance in broadening the applications of such membranes in many areas. Moreover, the addition of PEOX is expected to improve the water permeability and practical performance of the PSf asymmetric ultrafiltration membrane. The high hydrophilicity of PEOX might not only increase the hydrophilicity of the resulting PSf ultrafiltration membrane but might also increase the compatibility between the PSf casting solution and the coagulation bath (thereby, increasing the thermodynamic instability of the casting solution in the phase separation process). On the one hand, a hydrophilic membrane surface can prevent the adsorption of foulants, suggesting a better anti-fouling property.^{34,35} On the other hand, the phase separation mechanism may be more prone to instantaneous demixing, which will induce more macrovoid structures and thereby result in better water permeability.^{36,37}

Various combinations of PSf and PEOX dosages were adopted in this research in order to study the influence of PEOX on the phase separation mechanism and on the practical performance of the resulting ultrafiltration membranes.

2. Experimental section

2.1. Materials

PSf (Udel® P-3500, Solvay, China), average molecular weight of 22 000 g mol^{−1}, was used as the base polymer in the casting solution. *N,N*-Dimethylformamide (DMF) with analytical purity of 99.5%, purchased from Aladdin (China), was used as the solvent, and distilled water was used as the non-solvent. PEOX (purchased from Alfa Aesar, China) with an average molecular weight of 200 000 g mol^{−1} was used as the additive. Bull Serum Albumin (BSA) used to perform rejection property and anti-fouling property experiments was purchased from Aladdin (China). Hydrochloric acid (AR) and sodium hydroxide (AR), purchased from Aladdin (China), were used to adjust the pH value of feed solutions.

2.2. Preparation of the membranes

Asymmetric PSf membranes were prepared by a phase separation method. Different amounts of PEOX were added into the PSf/DMF matrix (the weight ratio of PSf in the cast solution was constant at 18 wt%) and dissolved at room temperature with magnetic stirring for at least 24 h to ensure that all PSf and PEOX were dissolved in DMF. The prepared solutions were poured into injectors and then kept them sealed and undisturbed overnight to eliminate air bubbles in solutions.

The casting solution was cast uniformly on a polyester film substrate by a hand-casting knife with a 250 μm knife gap. Then, the cast was immersed into a non-solvent (distilled water) bath immediately to complete the phase separation; the process needs to be done quickly because the moisture in the air can also lead to the phase separation process. After the casting



Table 1 The compositions of the casting solutions

Membranes	PEOX (wt%)	DMF (wt%)	PSf (wt%)
M-0	0	82	18
M-0.5	0.5	81.5	18
M-1	1.0	81	18
M-2	2.0	80	18
M-3	3.0	79	18

solution was immersed into the non-solvent (distilled water) bath, an exchange between the solvent (DMF) and the non-solvent (distilled water) was induced. The coagulation bath temperature (CBT) of 25 °C was selected in our experiments.

When the phase separation process was done, the residual DMF in membranes was removed by transferring the membranes into another container with fresh distilled water, and then the membranes were kept in fridge at 4 °C and tested after 24 h. An overview of the compositions of different casting solutions is reported in Table 1. In this study, all the samples were named as M-X, where X corresponds to the amount of PEOX.

2.3. Characterization of the membranes

2.3.1. Solution viscosity measurements. Viscosities of the PSf solution and PSf/PEOX solutions were measured using a rotational viscometer (Model NDJ-1, Shanghai balance instruments factory, China) at a constant temperature of 25 °C.

2.3.2. Phase separation kinetics. An optical microscope (ECLIPSE LV100N POL, Nikon, Japan) with a digital camera (MC56, MICROSHOT, Singapore) was used to investigate the phase separation kinetics during the membrane precipitation process.³⁸⁻⁴⁰

In this experiment, a drop of PSf solution, around 10 μL, was placed on a glass slide and covered with a hydrophilic coverslip as fast as possible to prevent any phase separation of PSf solution in air. The sample was moved to the optical microscope; the magnification was set at 50×. A drop of distilled water was added to the edge of the coverslip, and phase separation occurred when the water came into contact with the PSf solution. The forward velocity of the moving boundary was measured by the optical microscope; images were taken every 5 s. The formula for phase separation kinetics was as shown below:

$$X = 2(D_e t)^{1/2} \quad (1)$$

where, D_e is the diffusion factor ($\text{mm}^2 \text{ s}^{-1}$), X is the phase separation distance (mm), and t is the coagulation time (s).

In this research, the kinetics of membrane formation was studied. The thermodynamic and rheological variation of the PSf solution affected by the addition of PEOX has been discussed.

2.3.3. Scanning electron microscopy (SEM). The morphologies of top surface and cross-section of PSf membranes were observed with a HITACHI S-4800 SEM (Japan). In order to survey the morphology of cross-section fraction, membranes were

fractured in liquid nitrogen, and the fracture surfaces were carefully protected. Top surface samples and cross-section samples were coated with thin film of gold by sputtering before testing.

2.3.4. Chemical structure characterization. Fourier transform infrared spectroscopy (FTIR) (Nicolet iS 50 FT-IR, Thermo Fisher Scientific, USA) was adopted to determine the chemical structure of the PSf UF membrane and PSf/PEOX UF membranes by using the ATR (attenuated total reflectance) method. The top surface of samples was tested in our experiments. Transmittance spectra ranged from 650 to 4000 cm^{-1} .

2.3.5. Porosity measurements. A dry-wet weight method was adopted to measure the membrane porosity. The membranes were taken out of the distilled water bath and the superficial water was mopped by a high-pressure air knife. Then, the wet membranes were weighed and marked as wet weights (W_w). After that, membranes were first dried in an air-circulating oven at 60 °C for 24 h and then dried in a vacuum oven at 80 °C for the subsequent 24 h. Then, the membranes were weighed and marked as dry weights (W_d). The porosity of membrane was calculated using the following equation:

$$P (\%) = \frac{W_w - W_d}{\rho_w \times S \times \delta} \times 100 \quad (2)$$

where, $P (\%)$ is the porosity of membrane, W_w (g) and W_d (g) are the sample's wet weight and dry weight, respectively. ρ_w (g cm^{-3}) is the density of pure water at the testing temperature, S (cm^2) is the area of the membrane while δ (cm) is the thickness of the membrane in the wet state. To ensure data accuracy and repeatability, minimum three tests were performed for each membrane and the average was calculated.

2.3.6. Contact angle (CA) tests. The contact angles (CA) of the membranes were tested on a contact angle instrument (K100; KRÜSS; Germany). The membranes were dried in an air-circulating oven at 60 °C for 24 h before testing. Next, a water droplet of 4 μL was placed on the top surface of each membrane. Then, the contact angle of the droplet with the surface of the membrane was measured. Five repeated trials were carried out for each sample.

2.3.7. Pure water flux (PWF) and rejection measurements. The PWF measurement was carried out on a flat membrane filtration experimental instrument (FlowMen0021-HP, FMT, China); distilled water was fed at a transmembrane pressure of 0.25 MPa at 25 ± 0.1 °C. The effective testing area of the membrane was 120 cm^2 . The PWF was calculated using the following equation:⁴¹

$$\text{PWF} = \frac{V}{S \times t} \quad (3)$$

where, PWF ($\text{L m}^{-2} \text{ h}^{-1}$) is the pure water flux, V (L) is the permeate volume, S (m^2) is the membrane area, and t (h) is the sampling time. To ensure data accuracy and repeatability, at least three valid tests were performed for each membrane.

The rejection property of a membrane was tested with a 200 mg L⁻¹ BSA solution (in 0.1 M phosphate-buffer solution (PBS), pH = 7.0), and the solution was fed at a transmembrane pressure of 0.25 MPa at 25 ± 0.1 °C. Distilled water was filtered



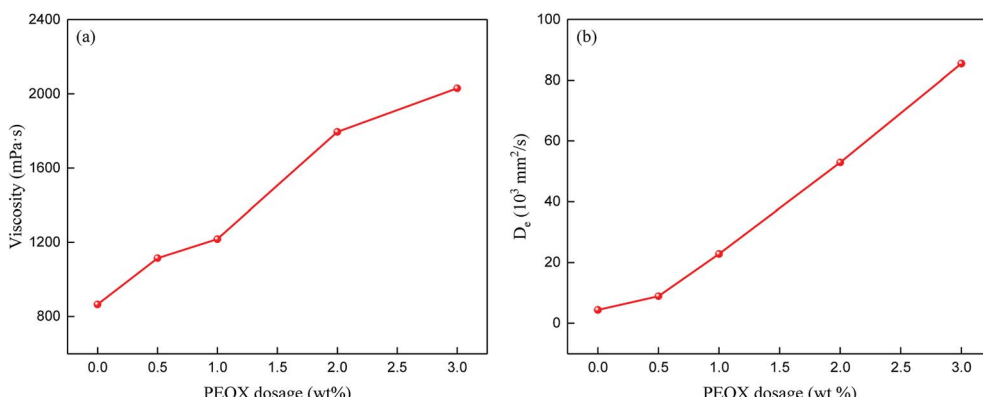


Fig. 1 The viscosities and effective diffusion coefficients of PSf solutions with various PEOX dosages. (a) Viscosities of PEOX solutions; (b) effective diffusion coefficients of PEOX solutions.

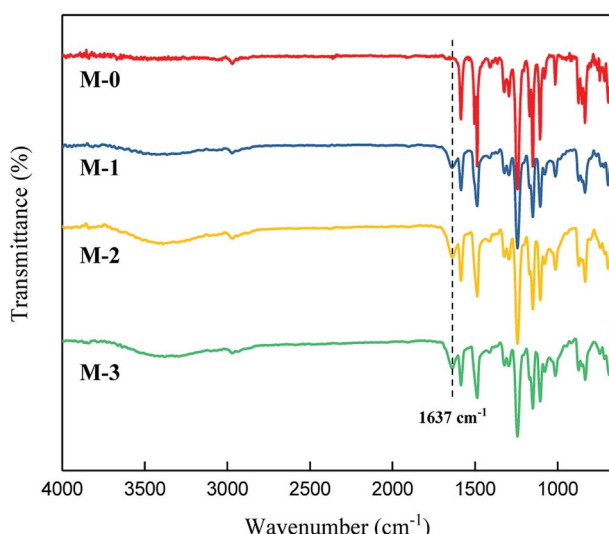


Fig. 2 ATR-FTIR spectra of the membranes.

through the membranes before the rejection testing, until the flux was stable. The BSA concentrations before and after testing were determined by an ultraviolet-visible spectrophotometer (TU-1900; Beijing Purkinje General Instrument Co., Ltd; China). The absorbance at the wavelength of 205 nm was read to estimate the BSA concentration. The rejection rates were calculated according to the following equation:

$$R = 1 - \frac{C_a}{C_b} \quad (4)$$

where, R (%) is the rejection rate, C_a is the concentration of BSA after testing, and C_b is the concentration of BSA before testing. In the permeation tests, the water flow was set constant at 7.0 L min^{-1} . The rejection rate was obtained when the water flux was stable; the rejection results reflected the initial rejection for each membrane.

2.3.8. Anti-fouling test. The anti-fouling property of PSf ultrafiltration membranes was tested in our research. BSA was selected as the model foulant. A 1000 mg L^{-1} BSA solution (in 0.1 M PBS, pH = 7.0) was used as the feed solution at

a transmembrane pressure of 0.25 MPa at $25 \pm 0.1^\circ\text{C}$. The water flow was set as 7.0 L min^{-1} . The flux of the membrane was recorded.

The anti-fouling property was quantitatively analyzed, and the total flux decline ratio (DR_t) and flux recovery ratio (FRR) were calculated as follows:

$$\text{DR}_t = \frac{f_1 - f_\Delta}{f_1} \times 100\% \quad (5)$$

$$\text{FRR} = \frac{f_2}{f_1} \times 100\% \quad (6)$$

where, f_1 is the initial water flux of each sample, f_Δ is the flux of each sample after testing with the foulant feed solutions for 1 h, f_2 is the recovery water flux.

3. Results and discussions

3.1. Kinetic study

The membrane-forming process includes the shrinking and merging of the polymer phase. The morphology of the membranes is controlled and affected by the rate of the demixing process, which is divided into two forms: instantaneous demixing and delayed demixing.

During instantaneous demixing process, due to the high exchange rate of solvent and non-solvent, precipitation of the polymer phase completes instantly which results in the formation of a thick membrane with macrovoids and loose top surface. Low concentration of the polymer phase in the sublayer gives the non-solvent enough time to form nuclei and grow, and the macrovoids are therefore formed.

In the process of delayed demixing, nucleation and precipitation occur slowly, and there is enough time for the polymer phase to shrink and merge. The shrinking and merging of the polymer phase lead to a high polymer concentration at the top surface and in the sublayer, resulting in a dense top surface and thin membranes. Besides, in the delayed demixing process, free growth of limited nuclei is prevented, as is the merging of nuclei. So, the number of nuclei is large; however, they are distributed in the polymer film and lead to a less porous



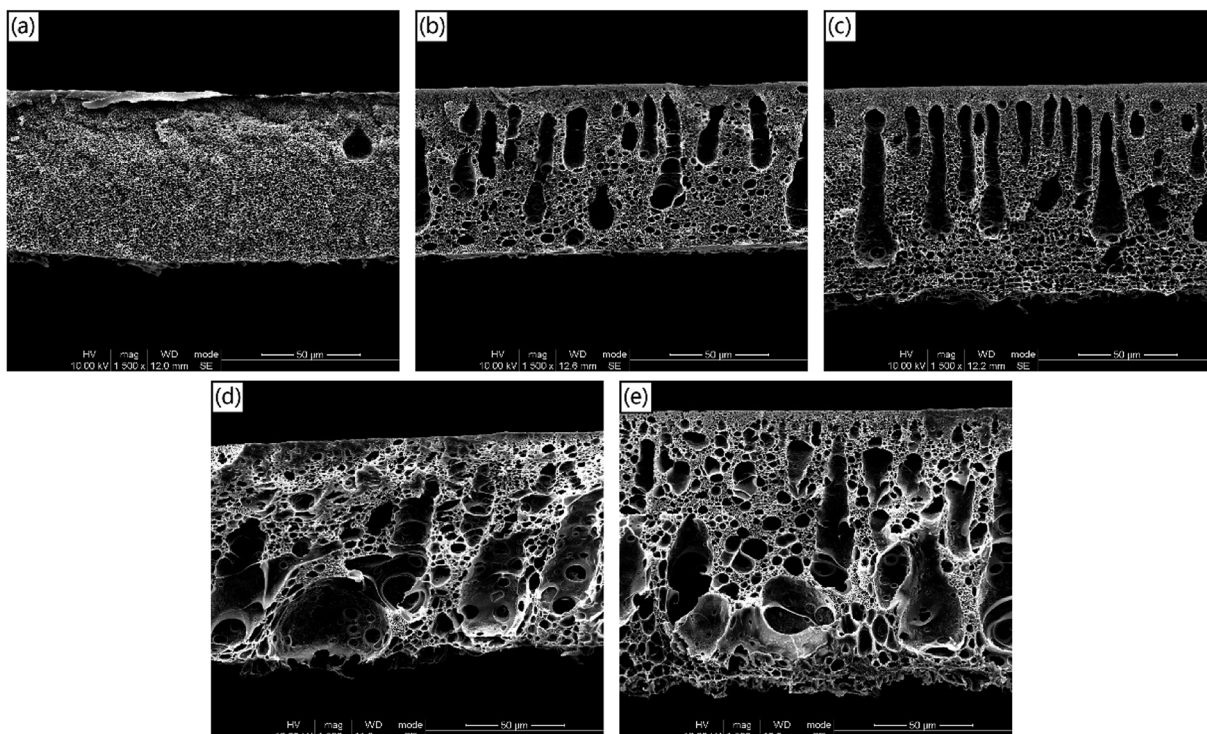


Fig. 3 The cross-sectional morphologies of the PSf/PEOX membranes with different PEOX dosages. (a) M-0; (b) M-0.5; (c) M-1; (d) M-2; (e) M-3.

structure with microvoids. Consequently, delayed demixing is the reverse of instantaneous demixing, often resulting in thinner and denser membranes.^{10,14,42}

The addition of polymer additive into the PSf casting solution may change the phase separation rate. In order to reveal the effect of PEOX on the phase separation kinetics of PSf solution,

the viscosities and effective diffusion coefficients of the PSf casting solutions were tested. The results are shown in Fig. 1. The results reveal that the addition of PEOX increases the viscosity of PSf solution. In general, the increasing viscosity of the casting solution always makes the phase separation kinetics more prone to delayed demixing. However, the effective

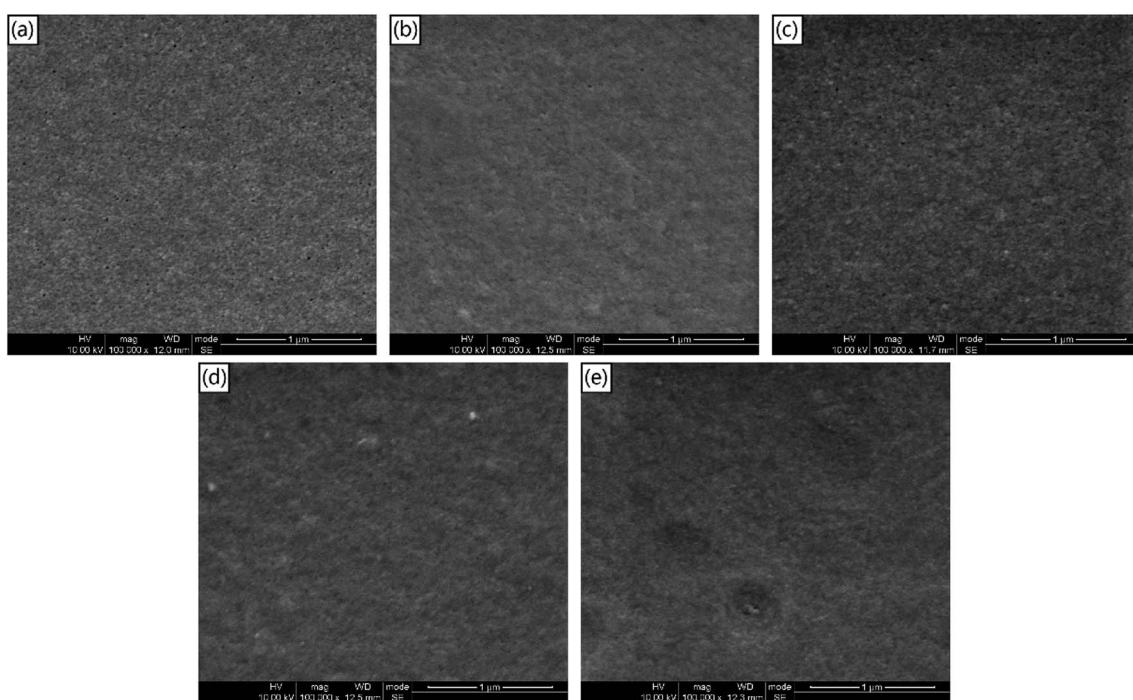


Fig. 4 The top surface morphologies of the PSf/PEOX membranes with different PEOX dosages. (a) M-0; (b) M-0.5; (c) M-1; (d) M-2; (e) M-3.

diffusion coefficient test shows an opposite result. The addition of PEOX drastically increases the diffusion rate during phase separation. This may be due to the high hydrophilicity of PEOX, which can improve the thermodynamic instability of the casting solution. Thus, the exchange rate between the solvent and non-solvent can be accelerated efficiently during the phase separation process.³⁶ The above results suggest that the phase separation process is more prone to instantaneous demixing.

3.2. Characterization of the membranes

ATR-FTIR has been adopted to determine the chemical structures of the polysulfone membranes. The results are shown in Fig. 2. Bands at 1242 cm^{-1} , 1487 cm^{-1} (aromatic ring breathing in the PSf chain⁴³) and 1584 cm^{-1} are characteristics of the polysulfone chain.⁴⁴ The identical absorption peaks of the primary amide groups (on the PEOX molecular chain) at 1637 cm^{-1} indicated that PEOX exists in all the PSf/PEOX membranes. The peak height of 1637 cm^{-1} increases along with the increased dosage of PEOX, indicating that more PEOX exists in the polymer matrix with the increase in PEOX dosage.

3.3. Morphological study

The structure and morphology of the asymmetric PSf/PEOX membranes affected by various PEOX dosages were explored by an SEM method.

SEM cross-sectional images of the PSf membranes with different PEOX dosages are depicted in Fig. 3. The incorporation of PEOX increases the thickness of the PSf membrane and induces the formation of macrovoids. The SEM images of the cross-section suggest that the presence of PEOX makes the phase separation process more prone to instantaneous demixing. The results are in agreement with the effective diffusion coefficient results in Fig. 1.

Fig. 4 shows the SEM images of the top surfaces of different membranes prepared with different PEOX dosages. It reveals that in a unit area of the membrane surface, both the visible number and the size of pores decrease with the increasing PEOX dosage. When the PEOX dosage is 3.0 wt% (M-3), the pores are too small to be recognized.

The top surface (skin layer) of a PSf membrane is formed by the imperfect merging of the PSf molecular chains.^{45,46} The addition of PEOX may decrease the pore size on the top surface because a more instantaneous demixing tendency suggests less inadequate merging time for the PSf phase. So, a better rejection rate is expected.

3.4. Porosity and contact angle (CA)

For an ultrafiltration membrane, its porosity and hydrophilicity are two crucial factors determining the membrane's permeability and rejection property. In the following sections, performances of PSf/PEOX membranes including porosity, contact angle, pure water flux (PWF) and rejection property were studied.

Porosity of the membranes (shown in Fig. 5) increases gradually with the increasing PEOX dosage; the results are in agreement with the SEM images. High porosity means low

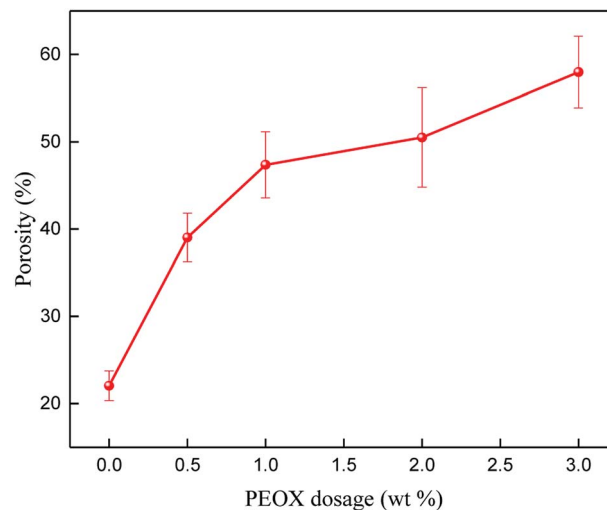


Fig. 5 The porosities of PSf/PEOX membranes with different PEOX dosages.

hydraulic resistance of a membrane, suggesting high hydraulic permeability.

The contact angles (CA) of PSf/PEOX membranes with different PEOX dosages are exhibited in Fig. 6. It can be seen that the CA is around 78° for a pure PSf membrane, which gradually decreases with the increase in PEOX dosages to around 61° for a membrane with 3.0 wt% PEOX. This is mainly because the dispersion of hydrophilic PEOX in the membrane matrix leads to the decrease in CA.

3.5. Pure water flux (PWF) and rejection measurements

Pure water flux (PWF) and rejection property are the key practical performance parameters for any membrane.⁴⁷ The PWF and the rejection property have a trade-off in almost all kinds of membranes; in general, a membrane with high PWF has a low rejection, and *vice versa*. For an ultrafiltration membrane, its

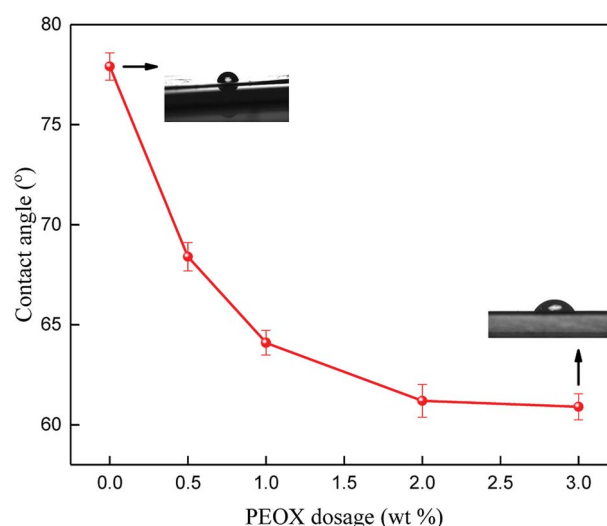


Fig. 6 The contact angles (CA) of PSf/PEOX membranes with different PEOX dosages.

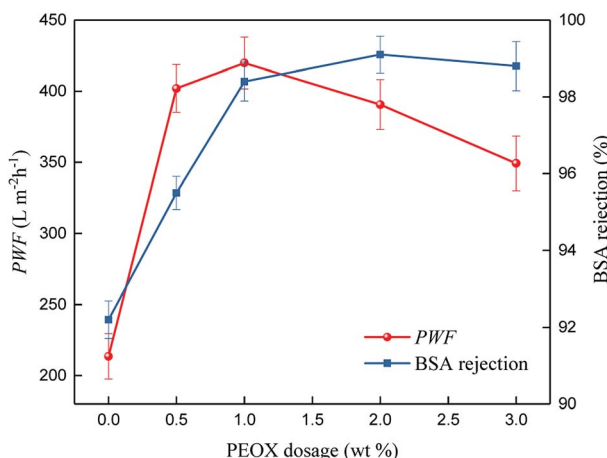


Fig. 7 Effect of PEOX dosage on the permeability of PSf/PEOX membranes.

PWF and rejection rates are determined by the number and size of pores on the top surface of the membrane, and the permeation mechanism is based on size exclusion.^{19,48} The effects of PEOX dosage on PWF and protein rejection are presented in Fig. 7.

The PWF of a pure PSf membrane is $213.5 \text{ L m}^{-2} \text{ h}^{-1}$. When the dosage of PEOX increases, PWF increases accordingly. Particularly, the PWF can reach $419.8 \text{ L m}^{-2} \text{ h}^{-1}$ when the dosage of PEOX is 1.0 wt%, around 197% higher than that of the original PSf membrane. The BSA rejection by the resulting membranes also increases with the increase in PEOX dosage, and reaches more than 98.4% when the dosage of PEOX is 1.0 wt% and higher.

The results suggest that the practical performance of the resulting ultrafiltration membrane is drastically improved. According to the permeation mechanism, the rejection of BSA is mainly affected by the pores' size, and the rejection mechanism is affected by pore selection, *i.e.* smaller pores indicate better rejection.¹⁹

Moreover, the improvement in PWF is not disproportionate with the increase in CA. This correlation suggests that although the top surface pores become small, the increase in number of macrovoids and hydrogen bond interactions lead to the improvement of PWF. However, porosity of the top surface pore is hard to measure directly, but it can be tested indirectly *via* the flux and rejection measurements. With the continued increase in PEOX dosage, the PWF begins to decline, which may be because of the shrinkage of the top surface pores.

Commonly, the addition of hydrophilic additive, such as PEG, can double the water flux of the resulting membrane when the dosage of PEG is around 10 wt%, while the BSA rejection will decline.⁴⁷ However, in our research, only a small dosage of PEOX (1.0 wt%) can double the water flux of the membrane and increase the BSA rejection.

In addition, the pH value-responsive property of the resulting UF membrane was tested. The permeabilities of PSf/PEOX membranes were tested using feed solutions with various pH

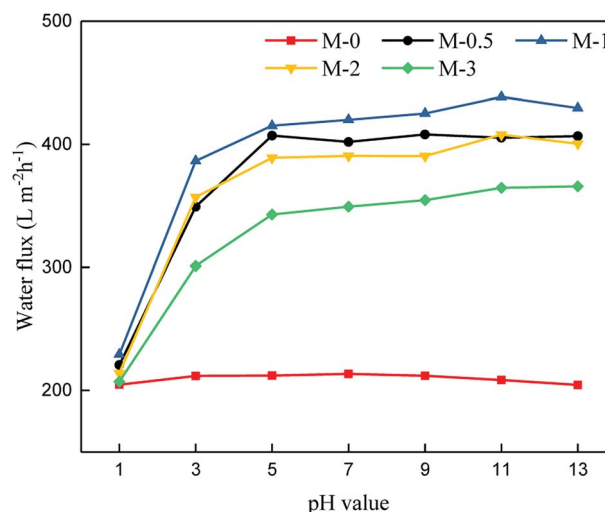


Fig. 8 pH value-responsive property of the resulting UF membranes.

values ranging from 1.0–13.0. The fluxes of the membranes are shown in Fig. 8.

From Fig. 8, the pH value is observed to have little effect on the permeation property of the pure PSf UF membrane. Interestingly, the water fluxes of the PSf/PEOX UF membranes varies along with the change in pH value of the feed solution. When the pH value is 1.0, the PSf/PEOX UF membranes show a low water flux, which is similar to the water flux of a pure PSf UF membrane. As the pH value increases, the water fluxes of PSf/PEOX UF membranes improve significantly from around $200 \text{ L m}^{-2} \text{ h}^{-1}$ to $400 \text{ L m}^{-2} \text{ h}^{-1}$.

The change in water flux of the membrane may be attributed to the change in hydrogen bonding reactions between the PEOX chains and water. When the pH value is low, the amide groups in PEOX are ionized,^{30,31,49} and the PEOX molecular chains may aggregate *via* intermolecular hydrogen bonds. So, the hydrogen bonding between the PEOX chains and water becomes weak. The smaller surface pore size causes the PSf/PEOX UF membranes to have a similar water flux compared with that of the pure PSf UF membrane. When the pH value increases, the hydrogen bonding interaction between PEOX chains becomes weak, and that between PEOX chains and water becomes strong. As a result, the water fluxes of PSf/PEOX UF membranes increase because of the strong hydrogen bonding interactions between the membranes and water.³¹ The pH value-responsive property is found to be repeatable in our experiments.

This interesting pH-responsive behavior of the PSf/PEOX UF membrane has not been reported before, which broadens the application potential of the membrane in many specific cases.

3.6. Anti-fouling properties

BSA was selected as the model foulant to simulate the protein foulants in this research; the anti-fouling results of the membranes were shown in Fig. 9. The DR_t and FRR values were shown in Table 2. After 1 h of filtration, the flux of M-0 reduced to around 71% of the initial flux. However, the flux of PSf/PEOX membranes only reduced to around 84–87% of the initial flux.



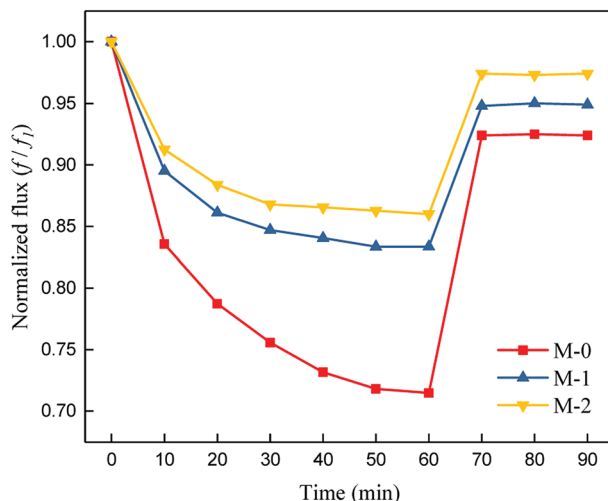


Fig. 9 Flux decline behavior of neat PSf and PSf/PEOX membranes during BSA filtration.

Table 2 Anti-fouling properties of the membranes

	M-0	M-1	M-2
DR _t (%)	28.5 ± 0.3	16.6 ± 0.5	14.0 ± 0.4
FRR (%)	92.4	94.8	97.4

In addition, the FRR of a PSf/PEOX membrane is better than that of the neat PSf membrane.

Membrane fouling can be affected by back transport, permeation drag and chemical interactions between the membrane and the foulants.⁵⁰ Since the test conditions for all membranes were the same, the different results mean that the interactions between the membranes and foulants became weak. The incorporation of PEOX makes the resulting PSf/PEOX UF membrane more hydrophilic than the pure PSf membrane. Therefore, the adsorption between the membrane and the foulants was reduced.

4. Conclusion

In this study, asymmetric polysulfone (PSf) and polysulfone/poly(2-ethyl-2-oxazoline) (PSf/PEOX) membranes were prepared by a phase separation method. PEOX was used at different dosages (0 wt%, 0.5 wt%, 1.0 wt%, 2.0 wt%, 3.0 wt%) as the polymeric additive in the casting solution. The effects of PEOX dosage on the phase separation kinetics, chemical properties, morphology, hydrophilicity, porosity and performances such as PWF, BSA rejection, pH value-responsiveness and anti-fouling property of the membranes were investigated in detail. The conclusions can be drawn as follows:

Results of the viscosities and effective diffusion coefficients of PSf/PEOX solutions combined with the SEM morphology observations revealed that, after the addition of PEOX, the casting solution showed more thermodynamic instability, while the resulting membrane became thicker with more macrovoids, indicating that the incorporation of PEOX makes the phase

separation process of the casting solution more prone to instantaneous demixing.

Hydrophilicity, pure water flux, BSA rejection and anti-fouling property of membranes have been improved significantly after the incorporation of PEOX. The PWF increases to 419.8 L m⁻² h⁻¹ when the dosage of PEOX is 1.0 wt% from the initial value of 213.5 L m⁻² h⁻¹ for the pure PSf membrane. BSA rejection by the resulting membranes increases with the increase in PEOX dosage, and reaches more than 98.4% when the dosage of PEOX is 1.0 wt% and higher.

The resulting PSf/PEOX UF membranes show an interesting pH value-responsive property, where the water flux changes along with the change in pH value of the feed solution. When the pH value of the feed solution is low, the water flux of the membrane declines; however, while the pH value of the feed solution increases, the water flux of the membrane improves significantly. This interesting feature of the membrane broadens the application potential of the membrane in many specific cases.

Conflicts of interest

There are no conflicts of interest to declare.

Acknowledgements

We gratefully acknowledge the National Natural Science Foundation of China (NSFC 51503134, 51421061, 51702282), the State Key Laboratory of Polymer Materials Engineering (Grant No. SKLPM 2017-3-02) for the financial support.

References

1. K. Scott, *Handbook of industrial membranes*, Elsevier, 1995.
2. E. Saljoughi, M. Amirilargani and T. Mohammadi, Effect of PEG additive and coagulation bath temperature on the morphology, permeability and thermal/chemical stability of asymmetric CA membranes, *Desalination*, 2010, **262**(1), 72–78.
3. P. Moradihamedani, N. A. Ibrahim, W. M. Z. W. Yunus and N. A. Yusof, Separation of CO₂ from CH₄ by pure PSF and PSF/PVP blend membranes: effects of type of nonsolvent, solvent, and PVP concentration, *J. Appl. Polym. Sci.*, 2013, **130**(2), 1139–1147.
4. V. Deimede, K. Nikitopoulou, A. Voege and J. Kallitsis, Study of polymer blend membranes composed of sulfonated polysulfone and PEO-grafted aromatic polyether with controllable morphology, *Eur. Polym. J.*, 2015, **63**, 113–122.
5. J. Wijmans, J. Baaij and C. Smolders, The mechanism of formation of microporous or skinned membranes produced by immersion precipitation, *J. Membr. Sci.*, 1983, **14**(3), 263–274.
6. R. Boom, I. Wienk, T. Van den Boomgaard and C. Smolders, Microstructures in phase inversion membranes. Part 2. The role of a polymeric additive, *J. Membr. Sci.*, 1992, **73**(2), 277–292.





7 C. Smolders, A. Reuvers, R. Boom and I. Wienk, Microstructures in phase-inversion membranes. Part 1. Formation of macrovoids, *J. Membr. Sci.*, 1992, **73**(2), 259–275.

8 Q.-Z. Zheng, P. Wang and Y.-N. Yang, Rheological and thermodynamic variation in polysulfone solution by PEG introduction and its effect on kinetics of membrane formation *via* phase-inversion process, *J. Membr. Sci.*, 2006, **279**(1), 230–237.

9 Q.-Z. Zheng, P. Wang, Y.-N. Yang and D.-J. Cui, The relationship between porosity and kinetics parameter of membrane formation in PSF ultrafiltration membrane, *J. Membr. Sci.*, 2006, **286**(1), 7–11.

10 E. Saljoughi, M. Amirilargani and T. Mohammadi, Effect of poly(vinyl pyrrolidone) concentration and coagulation bath temperature on the morphology, permeability, and thermal stability of asymmetric cellulose acetate membranes, *J. Appl. Polym. Sci.*, 2009, **111**(5), 2537–2544.

11 J. Mulder, *Basic principles of membrane technology*, Springer Science & Business Media, 2012.

12 J. Xu, Y. Tang, Y. Wang, B. Shan, L. Yu and C. Gao, Effect of coagulation bath conditions on the morphology and performance of PSf membrane blended with a capsaicin-mimic copolymer, *J. Membr. Sci.*, 2014, **455**(4), 121–130.

13 A. K. Hołda and I. F. J. Vankelecom, Integrally skinned PSf-based SRNF-membranes prepared *via* phase inversion—part A: influence of high molecular weight additives, *J. Membr. Sci.*, 2014, **450**(2), 512–521.

14 E. Saljoughi, M. Sadrzadeh and T. Mohammadi, Effect of preparation variables on morphology and pure water permeation flux through asymmetric cellulose acetate membranes, *J. Membr. Sci.*, 2009, **326**(2), 627–634.

15 A. Rahimpour and S. Madaeni, Polyethersulfone (PES)/cellulose acetate phthalate (CAP) blend ultrafiltration membranes: preparation, morphology, performance and antifouling properties, *J. Membr. Sci.*, 2007, **305**(1), 299–312.

16 E. Saljoughi and T. Mohammadi, Cellulose acetate (CA)/polyvinylpyrrolidone (PVP) blend asymmetric membranes: preparation, morphology and performance, *Desalination*, 2009, **249**(2), 850–854.

17 I. Wienk, R. Boom, M. Beerlage, A. Bulte, C. Smolders and H. Strathmann, Recent advances in the formation of phase inversion membranes made from amorphous or semicrystalline polymers, *J. Membr. Sci.*, 1996, **113**(2), 361–371.

18 H.-T. Yeo, S.-T. Lee and M.-J. Han, Role of a polymer additive in casting solution in preparation of phase inversion polysulfone membranes, *J. Chem. Eng. Jpn.*, 2000, **33**(1), 180–184.

19 M.-J. Han and S.-T. Nam, Thermodynamic and rheological variation in polysulfone solution by PVP and its effect in the preparation of phase inversion membrane, *J. Membr. Sci.*, 2002, **202**(1), 55–61.

20 B. Jung, J. K. Yoon, B. Kim and H.-W. Rhee, Effect of molecular weight of polymeric additives on formation, permeation properties and hypochlorite treatment of asymmetric polyacrylonitrile membranes, *J. Membr. Sci.*, 2004, **243**(1), 45–57.

21 D. Mosqueda-Jimenez, R. Narbaitz, T. Matsuura, G. Chowdhury, G. Pleizier and J. Santerre, Influence of processing conditions on the properties of ultrafiltration membranes, *J. Membr. Sci.*, 2004, **231**(1), 209–224.

22 T. P. Hou, S. H. Dong and L. Y. Zheng, The study of mechanism of organic additives action in the polysulfone membrane casting solution, *Desalination*, 1991, **83**(125), 343–360.

23 J.-H. Kim and K.-H. Lee, Effect of PEG additive on membrane formation by phase inversion, *J. Membr. Sci.*, 1998, **138**(2), 153–163.

24 J.-J. Shieh, T.-S. Chung, R. Wang, M. Srinivasan and D. R. Paul, Gas separation performance of poly(4-vinylpyridine)/polyetherimide composite hollow fibers, *J. Membr. Sci.*, 2001, **182**(1), 111–123.

25 A. Idris, N. M. Zain and M. Noordin, Synthesis, characterization and performance of asymmetric polyethersulfone (PES) ultrafiltration membranes with polyethylene glycol of different molecular weights as additives, *Desalination*, 2007, **207**(1–3), 324–339.

26 B. Chakrabarty, A. Ghoshal and M. Purkait, Effect of molecular weight of PEG on membrane morphology and transport properties, *J. Membr. Sci.*, 2008, **309**(1), 209–221.

27 Z.-L. Xu, T.-S. Chung, K.-C. Loh and B. C. Lim, Polymeric asymmetric membranes made from polyetherimide/polybenzimidazole/poly(ethylene glycol)(PEI/PBI/PEG) for oil-surfactant-water separation, *J. Membr. Sci.*, 1999, **158**(1), 41–53.

28 I.-C. Kim and K.-H. Lee, Effect of poly(ethylene glycol) 200 on the formation of a polyetherimide asymmetric membrane and its performance in aqueous solvent mixture permeation, *J. Membr. Sci.*, 2004, **230**(1), 183–188.

29 L. D. Villano, R. Kommedal, M. W. Fijten, U. S. Schubert, R. Hoogenboom and M. A. Kelland, A study of the kinetic hydrate inhibitor performance and seawater biodegradability of a series of poly(2-alkyl-2-oxazoline)s, *Energy Fuels*, 2009, **23**(7), 3665–3673.

30 C.-H. Wang and G.-H. Hsue, New amphiphilic poly(2-ethyl-2-oxazoline)/poly(L-lactide) triblock copolymers, *Biomacromolecules*, 2003, **4**(6), 1487–1490.

31 C. H. Wang and G. H. Hsue, Synthesis and characterization of temperature- and pH-sensitive hydrogels based on poly(2-ethyl-2-oxazoline) and poly(D,L-lactide), *J. Polym. Sci., Part A: Polym. Chem.*, 2002, **40**(8), 1112–1121.

32 P. Lin, C. Clash, E. M. Pearce, T. K. Kwei and M. A. Aponte, Solubility and miscibility of poly(ethyl oxazoline), *J. Polym. Sci., Part A: Polym. Chem.*, 2010, **26**(3), 603–619.

33 K. Aoi and M. Okada, Polymerization of oxazolines, *Prog. Polym. Sci.*, 1996, **21**(1), 151–208.

34 H. Wu, J. Huang and Y. Liu, Polysulfone ultrafiltration membrane incorporated with Ag-SiO₂ nanohybrid for effective fouling control, *J. Water Health*, 2017, **15**(3), 341.

35 I. Pinna and B. D. Freeman, *Membrane formation and modification*, American Chemical Society, 2000.

36 D. M. Wang, F. C. Lin, T. T. Wu and J. Y. Lai, Formation mechanism of the macrovoids induced by surfactant additives, *J. Membr. Sci.*, 1998, **142**(2), 191–204.

37 C. A. Smolders, A. J. Reuvers, R. M. Boom and I. M. Wienk, Microstructures in phase-inversion membranes. Part 1. Formation of macrovoids, *J. Membr. Sci.*, 1992, **73**(2), 259–275.

38 H. Strathmann, K. Kock, P. Amar and R. W. Baker, The formation mechanism of asymmetric membranes, *Desalination*, 1975, **16**(2), 179–203.

39 S. K. Yong, K. H. Jin and Y. K. Un, Asymmetric membrane formation via immersion precipitation method. I. Kinetic effect, *J. Membr. Sci.*, 1991, **60**(2–3), 219–232.

40 H. J. Kim, R. K. Tyagi, A. E. Fouad and K. Ionasson, The kinetic study for asymmetric membrane formation via phase-inversion process, *J. Appl. Polym. Sci.*, 1996, **62**(4), 621–629.

41 M. Sivakumar, D. R. Mohan and R. Rangarajan, Studies on cellulose acetate-polysulfone ultrafiltration membranes: II. Effect of additive concentration, *J. Membr. Sci.*, 2006, **268**(2), 208–219.

42 T. Mohammadi and E. Saljoughi, Effect of production conditions on morphology and permeability of asymmetric cellulose acetate membranes, *Desalination*, 2009, **243**(1–3), 1–7.

43 J. Wang, R. Xu, F. Yang, J. Kang, Y. Cao and M. Xiang, Probing influences of support layer on the morphology of polyamide selective layer of thin film composite membrane, *J. Membr. Sci.*, 2018, **556**, 374–383.

44 K. Singh, P. G. Ingole, J. Chaudhari, H. Bhrambhatt, A. Bhattacharya and H. C. Bajaj, Resolution of racemic mixture of α -amino acid derivative through composite membrane, *J. Membr. Sci.*, 2011, **378**(1), 531–540.

45 R. Datta, S. Dechapanichkul, J. S. Kim, L. Y. Fang and H. Uehara, A generalized model for the transport of gases in porous, non-porous, and leaky membranes. I. Application to single gases, *J. Membr. Sci.*, 1992, **75**(3), 245–263.

46 P. Ingo and W. J. Koros, Gas-permeation properties of asymmetric polycarbonate, polyestercarbonate, and fluorinated polyimide membranes prepared by the generalized dry-wet phase inversion process, *J. Appl. Polym. Sci.*, 2010, **46**(7), 1195–1204.

47 Y. Ma, F. Shi, J. Ma, M. Wu, J. Zhang and C. Gao, Effect of PEG additive on the morphology and performance of polysulfone ultrafiltration membranes, *Desalination*, 2011, **272**(1), 51–58.

48 R. W. Baker, *Membrane Technology and Applications*, Metallurgical Transactions A, 2nd edn, 2004, vol. 6.

49 Y. Zhao, Y. Zhou, D. Wang, Y. Gao, J. Li, S. Ma, L. Zhao, C. Zhang, Y. Liu and X. Li, pH-responsive polymeric micelles based on poly(2-ethyl-2-oxazoline)-poly(D, L-lactide) for tumor-targeting and controlled delivery of doxorubicin and P-glycoprotein inhibitor, *Acta Biomater.*, 2015, **17**, 182–192.

50 H. Hua, N. Li, L. Wu, H. Zhong, G. Wu, Z. Yuan, X. Lin and L. Tang, Anti-fouling ultrafiltration membrane prepared from polysulfone-graft-methyl acrylate copolymers by UV-induced grafting method, *J. Environ. Sci.*, 2008, **20**(5), 565–570.

